In Vivo Labeling

DOI: 10.1002/anie.201304026

# Mesoporous Silica Nanoparticle Pretargeting for PET Imaging Based on a Rapid Bioorthogonal Reaction in a Living Body**

*Sang Bong Lee, Hye Lan Kim, Hwan-Jeong Jeong, Seok Tae Lim, Myung-Hee Sohn, and Dong Wook Kim**

Positron emission tomography (PET) plays an important role as an imaging method because it can provide biological information at the molecular level in a living system with excellent sensitivity.[1,2] The visualization of in vivo biological processes using PET requires the preparation of specific molecular imaging probes labeled with positron-emitting radioisotopes.[3,4] In this regard, fluorine-18 ($^{18}$F) is the most popular positron emitter because its chemical, physiological, and nuclear characteristics are excellent and easy to obtain.[5–8] On the other hand, the short half-life of $^{18}$F ($t_{1/2}$ = 109.8 min) makes it potentially unsuitable for preparing macromolecule-based imaging probes, such as antibodies and bioactive nanoparticles, by labeling with $^{18}$F for an in vivo PET study because these nanoparticles normally require a long bloodstream-circulation time in the body to allow specific uptake into the target cells or organs.[3–5]

A range of nanoscale materials are applicable in broader vision of nanomedicine and have attracted considerable interest in early diagnostics and therapy.[9–16] Well-designed nanoparticles with an optimal size can have enhanced permeability and retention (EPR) effects to accumulate in tumor tissue. These EPR effects can maximize their performance in targeted biomedical imaging or cancer therapy.[17–21] In recent years, among the various nanocomposite systems, MSNs have been investigated extensively for a variety of applications in drug and gene-delivery platforms,[22–24] bioimaging,[25,26] cell markers,[27,28] and other important biomedical studies owing to their unique and favorable features, such as a high-loading capacity of various therapeutic or imaging agents that result from large pore volume and their large surface area, low cytotoxicity, excellent biocompatibility and biochemical stability, facile surface modification potential, and multifunctionality.[29,30] Therefore, given the importance of MSNs as vehicles in the biomedical field, their pharmacokinetic studies can be an important topic for examining the efficacy and biosafety of MSNs by in vivo real-time tracking using a PET system. On the other hand, this study of nanoparticles including MSNs with PET can frequently show various limitations owing to the short half-life of positron-emitters, particularly $^{18}$F, complicated labeling procedures, and harsh reaction conditions, or a time-consuming multistep process including purification.[31,32]

In recent significant advances, strain-promoted alkyne azide cycloaddition (SPAAC), which is referred to as copper-free click chemistry, have been used widely as a rapid bioorthogonal conjugation method for a variety of biological applications, such as live-cell imaging, radioisotope labeling, and surface modification.[33–44] In particular, the SPAAC of aza-dibenzocyclooctynes (DBCO) with biomolecule-associated azides to azadibenzocyclooctatriazoles (DBCOT) showed good performance in a living system for these purposes.[45–48] Herein, we introduce an extremely efficient MSN pretargeting for PET imaging by a fast and bioorthogonal SPAAC reaction of DBCO-substituted MSNs, which are accumulated in the tumor site by the EPR effect, with a short half-life $^{18}$F-labeled azide in tumor-bearing mice.

MSNs with a size of 100–130 nm are known to be able to accumulate in a tumor through the EPR effect by Lu et al.[49] Therefore, a DBCO based PEGylated MSN (DBCO-PEG-MSNs) with size of 100–150 nm was designed and prepared (Scheme 1). Amine-functionalized MSNs ($NH_2$-MSNs) were prepared according to a previously reported procedure.[24,27] Then, amine-functionalized PEG-MSNs ($NH_2$-PEG-MSNs) were obtained by the PEGylation of $NH_2$-MSNs using two different chain-length *N*-hydroxylsuccinimide (NHS) functionalized PEGs (Fmoc-protected amine-$PEG_{24}$-NHS ester and MeO-$PEG_{12}$-NHS ester) following a Fmoc-deprotection reaction in the presence of piperidine. Considering the easy accessibility of $^{18}$F-labeled azide radiotracer, a DBCO group serving as an azide acceptor was introduced into the long chain PEG-amine moiety of $NH_2$-PEG-MSNs by the amide-formation reaction using a DBCO-NHS compound **1** to obtain DBCO-PEG-MSNs. After the SPAAC reaction of DBCO-PEG-MSNs with an azide compound containing a single sulfur atom, a sulfur elemental analysis showed that approximately 0.12 mmole of the DBCO moiety was tethered to per gram of the DBCO-PEG-MSN product (Supporting Information, Scheme S1). All of the MSN derivatives were characterized by transmission electron microscopy (TEM), $N_2$ adsorption–desorption and pore-size distribution analysis, X-

[*] S. B. Lee,[+] Prof. D. W. Kim
Department of Chemistry, Inha University
100 Inha-ro, Nam-gu, Incheon 402-751 (Korea)
E-mail: kimdw@inha.ac.kr
H. L. Kim,[+] Dr. H.-J. Jeong, Dr. S. T. Lim, Dr. M.-H. Sohn
Department of Nuclear Medicine, Cyclotron Research Center
Molecular Imaging and Therapeutic Medicine Research Center
Chonbuk National University Medical School
Jeonju, Jeonbuk 561-712 (Korea)

[+] These authors contributed equally to this work.

[**] This work was supported by the Nuclear Research & Development Program of the National Research Foundation of Korea (NRF) grant funded by the Korean government (MEST) (grant code: 2011-0006322 and 2011-0030952), the Conversing Research Center Program through the MEST (grant code: 2011K000705), and INHA University Research Grant (INHA-47397-01).

Supporting information for this article is available on the WWW under http://dx.doi.org/10.1002/anie.201304026.

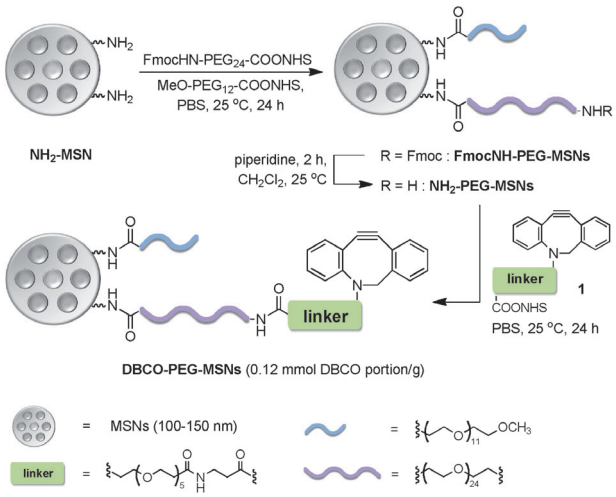


***Scheme 1.*** Preparation of DBCO-functionalized PEGylated mesoporous silica nanoparticles (MSNs). DBCO = aza-dibenocyclooctyne, PEG = polyethylene glycol.

ray powder diffraction (XRD), zeta potential and FTIR spectroscopy. These characteristic data suggest that all steps of MSNs had been synthesized successfully (Supporting Information, Figures S1–S5).

To investigate the SPAAC reaction rate and the possibility of the reaction-proceeding in an in vivo system, we attempted to conduct the model bioorthogonal SPAAC reaction of DBCO-PEG-MSNs (4 mg, 0.48 μmol of DBCO portion) with 11.1 MBq (specific radioactivity: 42 GBq μmol$^{-1}$) of [$^{18}$F]fluoropentaethylene glycolic azide ([$^{18}$F]**2**, prepared according to our previous work)[41] under the physiologically similar conditions (in PBS, pH 7.4, 36.5 °C) as shown in Figure 1. Under these reaction conditions, the SPAAC reaction proceeded rapidly and was completed within a reasonable reaction time (15–20 min), affording $^{18}$F-labeled azadibenzocyclooctatriazolic PEG-MSNs ($^{18}$F-DBCOT-PEG-MSNs) in almost quantitative radiochemical yield (RCY).

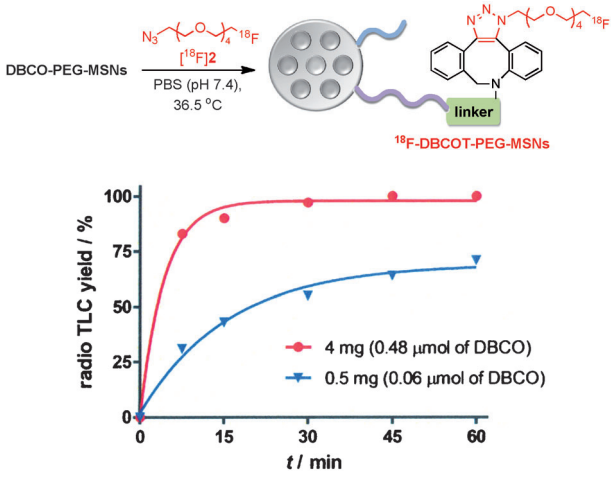


***Figure 1.*** Top: Model $^{18}$F-labeling reaction based on copper-free "click" SPAAC reaction under physiologically similar conditions (in PBS, pH 7.4, 36.5 °C). Bottom: Kinetic analysis of the SPAAC $^{18}$F-labeling reaction.

Moreover, the use of only 0.5 mg (0.06 μmol DBCO portion) of them allowed the same model reaction to provide the $^{18}$F-DBCOT-PEG-MSNs in more than 70 % RCY within 1 h. This suggests that this bioorthogonal SPAAC $^{18}$F-labeling reaction would show a good performance in an in vivo system.

Two findings, namely the rapid SPAAC reaction rate under biocompatible conditions and the localization of the MSNs in tumor by the EPR effect, prompted a further MSN-based pretargeting study using short half-life $^{18}$F based on SPAAC covalent labeling in an in vivo system. Figure 2 A shows the procedure for the DBCO-PEG-MSN-based pretargeting for PET imaging with $^{18}$F-labeled azide [$^{18}$F]**2** radiotracer, which is expected to have no targeting capability to the tumor cells when used alone, using a microPET-CT system. DBCO-PEG-MSNs (250 μg, 30 nmol DBCO portion) were injected intravenously into female nude mice bearing a subcutaneous U87 MG tumor on their right front leg. After 24 h, 2.6 MBq of [$^{18}$F]**2** was administered. Another group of mice was given the same dose of [$^{18}$F]**2** alone without previously administering the DBCO-PEG-MSNs (non-pretargeted). One mouse from each group was used for the microPET-CT imaging study at 15, 30, 60, and 120 min intervals after the injection of [$^{18}$F]**2**, thus considering the circulation and SPAAC reaction time of [$^{18}$F]**2** in the body. PET-CT images showed a persistently strong tumor signal in the mice given DBCO-PEG-MSNs 24 h earlier (the pretargeted mouse, Figure 2 C), whereas the non-pretargeted mouse given only [$^{18}$F]**2** alone had considerably less tumor uptake with a renal clearance of $^{18}$F activity (Figure 2 B). This in vivo imaging study demonstrated that, despite the lack of tumor targetability by [$^{18}$F]**2**, it could successfully visualize the tumor in vivo with high tumor accretion through the in situ synthesis of $^{18}$F-DBCOT-PEG-MSNs by a SPAAC reaction with the pretargeted DBCO-PEG-MSNs by the EPR effect at the tumor site.

The tissue distribution data from the necropsied mice confirmed the relationships derived from the PET imaging results at 120 min (Figure 3). The radiotracer [$^{18}$F]**2** showed a similar tissue distribution regardless of whether pretargeted or used alone, with the exception of the tumor, which had significantly high uptake in the DBCO-PEG-MSNs pretargeted mice compared to that in mice given the radiotracer alone. Furthermore, when 250 μg of DBCO-PEG-MSNs was used for pretargeting, the radiotracer exhibited a significantly higher tumor uptake than when 100 μg was used, thereby improving the tumor-to-nontumor ratios, and particularly the tumor-to-blood ratio. This dose-dependent pretargeting effect is good evidence of this hypothesis: bioorthogonal covalent $^{18}$F-labeling after tumor uptake of the nanoparticles by the EPR effect. Given the relatively high radioactivity in the blood from this necropsy data, high signal intensities were also observed in the head and neck area, which have a large blood pool, from both the non-pretargeting and pretargeting PET images. Additionally, considering that the unreacted [$^{18}$F]**2** was washed out by renal clearance, relatively high activity was observed in the urinary track area (kidney or bladder).

In summary, we have described an efficient MSN pretargeting for PET imaging based on the highly bioorthogonal

  

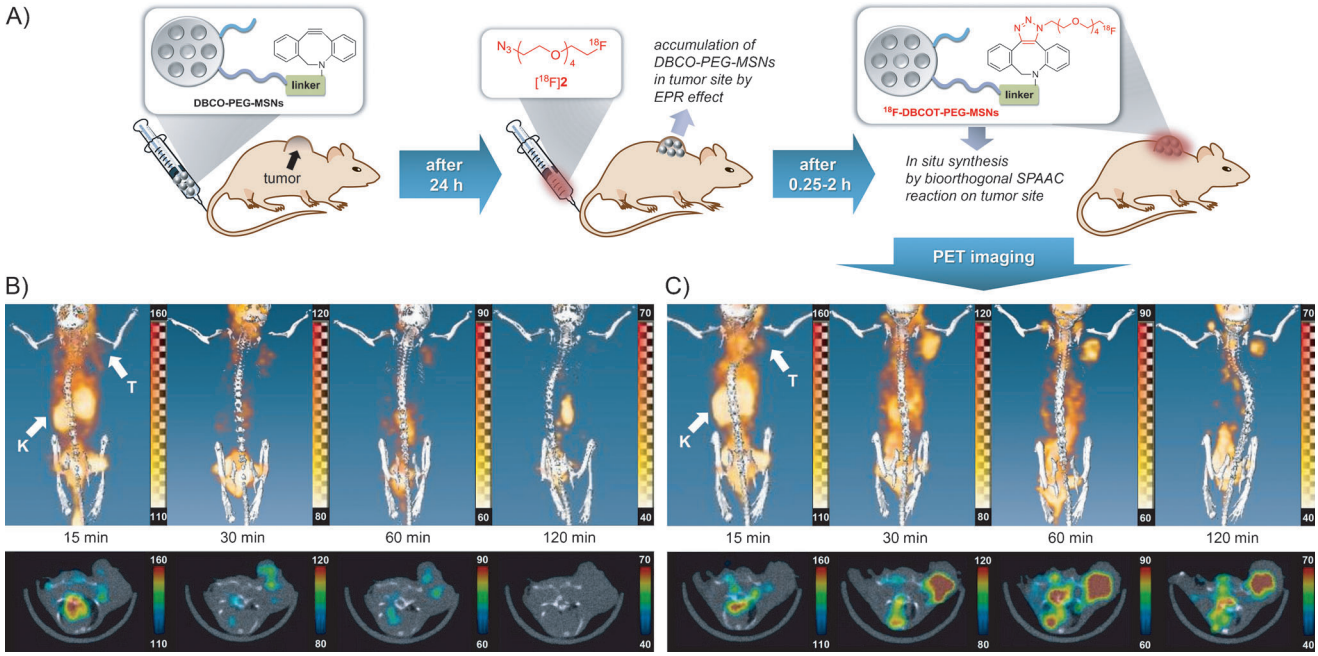


***Figure 2.*** Pretargeting PET imaging study by bioorthogonal covalent $^{18}$F-labeling. A) The procedure for the in situ synthesis of $^{18}$F-DBCOT-PEG-MSNs in a living specimen by a bioorthogonal SPAAC reaction for the DBCO-PEG-MSN-pretargeting PET-imaging study. B),C) Three-dimensional reconstruction (upper) and transverse section (lower) combined PET-CT images of $^{18}$F-labeled azide ([$^{18}$F]**2**; 2.6 MBq) in a U87 MG tumor-bearing mouse given only [$^{18}$F]**2** alone (non-pretargeted; B) or a mouse given DBCO-PEG-MSNs 24 h earlier (pretargeted; C) recorded at 15, 30, 60, and 120 min after injection of [$^{18}$F]**2**. T = tumor, K = kidneys.

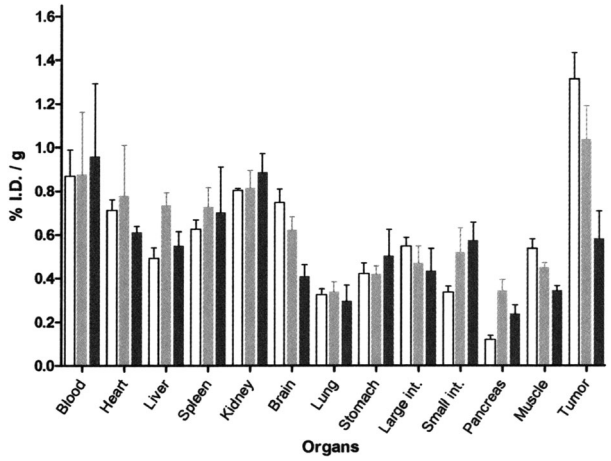


***Figure 3.*** Necropsy data. Biodistribution of [$^{18}$F]**2** in U87 MG tumor-bearing mice given 250 (white bars) or 100 μg (gray) of DBCO-PEG-MSNs 24 h earlier (pretargeted) and mice given only [$^{18}$F]**2** alone (black), at 2 h after injection. Data are expressed as normalized accumulation of activity in % ID/g ± SD ($n = 4$).

and rapid SPAAC conjugation reaction in a living system using fluorine-18. For this study, we prepared the DBCO-functionalized PEGylated MSNs, which can successfully accumulate in the tumor site by the EPR effect and react rapidly with an $^{18}$F-labeled azide synthon under physiologically similar reaction conditions. The successful application of this pretargeting approach was demonstrated by in vivo studies. In both PET imaging and necropsy data, the $^{18}$F-labeled azide radiotracer showed significantly high tumor uptake in the pretargeted mice by forming $^{18}$F-DBCOT-PEG-MSNs within 2 h after injection, by bioorthogonal covalent labeling, compared to that in the non-pretargeted mice. This pretargeting method is expected to assist in the field of drug delivery using MSNs with real-time monitoring by non-invasive imaging. Furthermore, given its speed and sensitivity in an in vivo system, we propose that this technology should enable PET molecular imaging studies with $^{18}$F with a short half-life as a PET radionuclide using other nanocomposite materials as well as macrobiomolecules (such as proteins and genes), which require a long bloodstream-circulation time in the body for specific uptake into the target cells or organs.

Further studies on the application of in vivo PET molecular imaging studies using various macrobiomolecules according to this procedure are currently underway.

Received: May 10, 2013
Revised: July 2, 2013
Published online: August 16, 2013

**Keywords:** bioorthogonal reactions · mesoporous silica · molecular imaging · nanoparticles · radiopharmaceuticals

[1] M. E. Phelps, *Proc. Natl. Acad. Sci. USA* **2000**, *97*, 9226 – 9233.
[2] T. F. Massoud, S. S. Gambhir, *Genes Dev.* **2003**, *17*, 545 – 580.
[3] S. Vallabhajosula, Molecular Imaging: Radiopharmaceuticals for PET and SPECT, 1 st ed., Springer, New York, **2009**.
[4] S. M. Ametamey, M. Honer, P. A. Schubiger, *Chem. Rev.* **2008**, *108*, 1501 – 1516.
[5] S. S. Gambhir, *Nat. Rev.* **2002**, *2*, 683 – 693.

  

[6] R. Schirrmacher, C. Wängler, S. Schirrmacher, *Mini-Rev. Org. Chem.* **2007**, *4*, 317 – 329.
[7] D. W. Kim, D.-S. Ahn, Y.-H. Oh, S. Lee, H. S. Kil, S. J. Oh, S. J. Lee, J. S. Kim, J. S. Ryu, D. H. Moon, D. Y. Chi, *J. Am. Chem. Soc.* **2006**, *128*, 16394 – 16397.
[8] P. W. Miller, N. J. Long, R. Vilar, A. D. Gee, *Angew. Chem.* **2008**, *120*, 9136 – 9172; *Angew. Chem. Int. Ed.* **2008**, *47*, 8998 – 9033.
[9] M. W. Ambrogio, C. R. Thomas, Y.-L. Zhao, J. I. Zink, J. F. Stoddart, *Acc. Chem. Res.* **2011**, *44*, 903 – 913.
[10] Z. Li, J. C. Barnes, A. Bosoy, J. F. Stoddart, J. I. Zink, *Chem. Soc. Rev.* **2012**, *41*, 2590 – 2605.
[11] A. S. L. Derycke, P. A. M. de Witte, *Adv. Drug Delivery Rev.* **2004**, *56*, 17 – 30.
[12] E. Amstad, E. Reimhult, *Nanomedicine* **2012**, *7*, 145 – 164.
[13] M. Lewin, N. Carlesso, C.-H. Tung, X.-W. Tang, D. Cory, D. T. Scadden, R. Weissleder, *Nat. Biotechnol.* **2000**, *18*, 410 – 414.
[14] Y.-w. Jun, J.-H. Lee, J. Cheon, *Angew. Chem.* **2008**, *120*, 5200 – 5213; *Angew. Chem. Int. Ed.* **2008**, *47*, 5122 – 5135.
[15] L. Lacerda, A. Bianco, M. Prato, K. Kostarelos, *Adv. Drug Delivery Rev.* **2006**, *58*, 1460 – 1470.
[16] A. de La Zerda, C. Zavaleta, S. Keren, S. Vaithilingam, S. Bodapati, Z. Liu, J. Levi, B. R. Smith, T.-J. Ma, O. Oralkan, Z. Cheng, X. Chen, H. Dai, B. T. Khuri-Yakub, S. S. Gambhir, *Nat. Nanotechnol.* **2008**, *3*, 557 – 562.
[17] G. M. Whitesides, *Nat. Biotechnol.* **2003**, *21*, 1161 – 1165.
[18] E. Katz, I. Willner, *Angew. Chem.* **2004**, *116*, 6166 – 6235; *Angew. Chem. Int. Ed.* **2004**, *43*, 6042 – 6108.
[19] D. Peer, J. M. Karp, S. Hong, O. C. Farokhzad, R. Margalit, R. Langer, *Nat. Nanotechnol.* **2007**, *2*, 751 – 760.
[20] R. Hao, R. Xing, Z. Xu, Y. Hou, S. Gao, S. Sun, *Adv. Mater.* **2010**, *22*, 2729 – 2742.
[21] a) L. Y. T. Chou, K. Ming, W. C. W. Chan, *Chem. Soc. Rev.* **2011**, *40*, 233 – 245; b) E. Ruoslahti, S. N. Bhatia, M. J. Sailor, *J. Cell Biol.* **2010**, *188*, 759 – 768; c) Z. Cheng, A. A. Zaki, J. Z. Hui, V. R. Muzykantov, A. Tsourkas, *Science* **2012**, *338*, 903 – 910.
[22] N. K. Mal, M. Fujiwara, Y. Tanaka, *Nature* **2003**, *421*, 350 – 353.
[23] T. Xia, M. Kovochich, M. Liong, H. Meng, S. Kabehie, S. George, J. I. Zink, A. E. Nel, *ACS Nano* **2009**, *3*, 3273 – 3286.
[24] C.-H. Lee, S.-H. Cheng, I.-P. Huang, J. S. Souris, C.-S. Yang, C.-Y. Mou, L.-W. Lo, *Angew. Chem.* **2010**, *122*, 8390 – 8395; *Angew. Chem. Int. Ed.* **2010**, *49*, 8214 – 8219.
[25] K. Taylor, J. Kim, W. Rieter, H. An, W. Lin, *J. Am. Chem. Soc.* **2008**, *130*, 2154 – 2155.
[26] C.-H. Lee, S.-H. Cheng, Y.-J. Wang, Y.-C. Chen, N.-T. Chen, J. Souris, C.-T. Chen, C.-Y. Mou, C.-S. Yang, L.-W. Lo, *Adv. Funct. Mater.* **2009**, *19*, 215 – 222.
[27] Y.-S. Lin, C.-P. Tsai, H.-Y. Huang, C.-T. Kuo, Y. Hung, D.-M. Huang, Y.-C. Chen, C.-Y. Mou, *Chem. Mater.* **2005**, *17*, 4570 – 4573.
[28] L. Pan, Q. He, J. Liu, Y. Chen, M. Ma, L. Zhang, J. Shi, *J. Am. Chem. Soc.* **2012**, *134*, 5722 – 5725.
[29] J. E. Lee, N. Lee, T. Kim, J. Kim, T. Hyeon, *Acc. Chem. Res.* **2011**, *44*, 893 – 902.
[30] J. M. Rosenholm, V. Mamaeva, C. Sahlgren, M. Lindén, *Nanomedicine* **2012**, *7*, 111 – 120.
[31] E. Andreozzi, J. W. Seo, K. Ferrara, A. Louie, *Bioconjugate Chem.* **2011**, *22*, 808 – 818.
[32] D. Zeng, N. S. Lee, Y. Liu, D. Zhou, C. S. Dence, K. L. Wooley, J. A. Katzenellenbogen, M. J. Welch, *ACS Nano* **2012**, *6*, 5209 – 5219.
[33] E. M. Sletten, C. R. Bertozzi, *Acc. Chem. Res.* **2011**, *44*, 666 – 676.
[34] M. F. Debets, S. S. van Berkel, J. Dommerholt, A. J. Dirks, F. P. J. T. Rutjes, F. L. van Delft, *Acc. Chem. Res.* **2011**, *44*, 805 – 815.
[35] J. C. Jewett, C. R. Bertozzi, *Chem. Soc. Rev.* **2010**, *39*, 1272 – 1279.
[36] N. K. Devaraj, R. Upadhyay, J. B. Haun, S. A. Hilderbrand, R. Weissleder, *Angew. Chem.* **2009**, *121*, 7147 – 7150; *Angew. Chem. Int. Ed.* **2009**, *48*, 7013 – 7016.
[37] S. T. Laughlin, J. M. Baskin, S. L. Amacher, C. R. Bertozzi, *Science* **2008**, *320*, 664 – 667.
[38] J. C. Jewett, E. M. Sletten, C. R. Bertozzi, *J. Am. Chem. Soc.* **2010**, *132*, 3688 – 3690.
[39] L. S. Campbell-Verduyn, L. Mirfeizi, A. K. Schoonen, R. A. Dierckx, P. H. Elsinga, B. L. Feringa, *Angew. Chem.* **2011**, *123*, 11313 – 11316; *Angew. Chem. Int. Ed.* **2011**, *50*, 11117 – 11120.
[40] R. Rossin, P. R. Verkerk, S. M. van den Bosch, R. C. M. Vulders, I. Verel, J. Lub, M. S. Robillard, *Angew. Chem.* **2010**, *122*, 3447 – 3450; *Angew. Chem. Int. Ed.* **2010**, *49*, 3375 – 3378.
[41] K. Sachin, V. H. Jadhav, E.-M. Kim, H. L. Kim, S. B. Lee, H.-J. Jeong, S. T. Lim, M.-H. Sohn, D. W. Kim, *Bioconjugate Chem.* **2012**, *23*, 1680 – 1686.
[42] A. Bernardin, A. Cazet, L. Guyon, P. Delannoy, F. Vinet, D. Bonnaffé, I. Texier, *Bioconjugate Chem.* **2010**, *21*, 583 – 588.
[43] a) B. M. Zeglis, P. Mohindra, G. I. Weissmann, V. Divilov, S. A. Hilderbrand, R. Weissleder, J. S. Lewis, *Bioconjugate Chem.* **2011**, *22*, 2048 – 2059; b) N. K. Devaraj, G. M. Thurber, E. J. Keliher, B. Marinelli, R. Weissleder, *Proc. Natl. Acad. Sci. USA* **2012**, *109*, 4762 – 4767.
[44] K. Lang, L. Davis, J. Torres-Kolbus, C. Chou, A. Deiters, J. W. Chin, *Nat. Chem.* **2012**, *4*, 298 – 304.
[45] X. Ning, J. Guo, M. A. Wolfert, G.-J. Boons, *Angew. Chem.* **2008**, *120*, 2285 – 2287; *Angew. Chem. Int. Ed.* **2008**, *47*, 2253 – 2255.
[46] A. A. Poloukhtine, M. A. Wolfert, N. E. Mbua, G.-J. Boons, V. V. Popik, *J. Am. Chem. Soc.* **2009**, *131*, 15769 – 15776.
[47] M. F. Debets, S. S. van Berkel, S. Schoffelen, F. P. J. T. Rutjes, J. C. M. van Hest, F. L. van Delft, *Chem. Commun.* **2010**, *46*, 97 – 99.
[48] B. R. Varga, M. Kállay, K. Hegyi, S. Béni, P. Kele, *Chem. Eur. J.* **2012**, *18*, 822 – 828.
[49] J. Lu, M. Liong, Z. Li, J. I. Zink, F. Tamanoi, *Small* **2010**, *6*, 1794 – 1805.

  